ELSEVIER

Journal of Nuclear Materials 289 (2001) 71–79

journal of nuclear materials

www.elsevier.nl/locate/jnucmat

Molecular dynamics refinement of topologically generated reconstructions of simulated irradiation cascades in silica networks

Xianglong Yuan [a], Vinay Pulim [b], Linn W. Hobbs [a,*]

[a] *Department of Materials Science and Engineering, Massachusetts Institute of Technology, Room 13-4054, 77 Massachusetts Avenue, Cambridge MA 02139-4307, USA*

[b] *Laboratory for Computer Science, Massachusetts Institute of Technology, Cambridge MA 02139-4307, USA*

Abstract

Silica irradiation cascade structures, simulated using topological modeling approaches, have been refined using molecular dynamics simulation techniques. Major structural reconstruction was observed when silica is equilibrated in this way at and above a glass transition temperature. Below the glass transition, irradiated cascades were found to have largely retained their original topological structures, and in this way several fully connected metastable silicas with substantially different medium-range structures were obtained. Analysis of these structures further revealed that their total correlation functions were remarkably insensitive to changes in their medium-range ring complement. Information in the first sharp diffraction peak (FSDP) is shown instead to provide some insight into the topologies of irradiated silicas.

PACS: 61.43. Bn; 61.43.Fs; 61.80.Az

1. Introduction

Silica and its allied silicates are the most abundant substances on earth. Various forms of silica form the constituents of many natural minerals. Radiation effects in silicas and silicate glasses have long been of interest, because of their wide use in many technological applications, such as in fiber optics, as optical lenses, in flat panel displays, as insulating layers in metal-oxide-semiconductor (MOS) devices, in frequency-control devices, and as nuclear waste storage media [1,2]. Displacive forms of radiation, for example, energetic neutrons or ions in whose wake atomic collision cascades are created, alter atomic arrangements in silicas and result in significant changes in properties and performance. Studies [3–6] of neutron-irradiated crystalline and vitreous silica have reported substantial structural alteration by irradiation, in particular reduction to non-crystalline states of common terminal density known geologically as *metamict* [7]. Though apparently comprising the same constituent vertex-sharing [SiO_4] tetrahedral units, these metamict structures differ from vitreous silica, and from pressure-densified silica of comparable density, both spectroscopically and energetically [8–10]. Here, the term 'metamict' (literally, rendered into an altered state) provides a preferable alternative to 'amorphized' for describing such irradiated structures that are effectively topologically disordered [11], since the radiation disordering can also proceed from an initially topologically disordered vitreous silica, for which the term 'amorphization' has little meaning.

While the structures of the crystalline polymorphs are well documented [12], the topologically disordered structure of even the exhaustively studied vitreous form of silica remains largely enigmatic, let alone the structures of other amorphous silicas. Diffraction unfortunately provides only average information about short-range order and is relatively insensitive to medium-range order differences [13].

* Corresponding author. Tel.: +1-617 253 6835; fax: +1-617 252 1020.

E-mail address: hobbs@mit.edu (L.W. Hobbs).

0022-3115/01/$ - see front matter
PII: S0022-3115(00)00703-0

A useful way is to envisage the possibilities for the tetrahedral arrangements in silicas topologically [11]. Crystalline silicas are easy to amorphize by irradiation because they possess sufficient topological freedom to be only marginally rigid [14]. Many forms of topological disorder can result because multiple stochastic reconstructive paths are available following the initial radiation-induced disordering. Topological modeling of irradiation collision cascades in a range of silica structures has been previously carried out using rules-based assembly and global maximal matching procedures [15–18]. In this study, we focus on the refinement of these radiation-induced topologically disordered models, using molecular dynamics (MD) simulation techniques, and investigate model stabilities at different simulation temperatures. We also analyze ring statistics, total correlation functions, and the position of the first sharp diffraction peak (FSDP) for the refined models for comparison to experimental results.

2. Computational procedures

In this study, three forms of collision cascade were initially simulated using topological modeling: (1) an α-quartz cascade reassembled using α-cristobalite topological assembly rules; (2) an α-quartz cascade reassembled by maximal global matching; and (3) a β-cristobalite cascade reassembled by maximal global matching. Details of the initial topological cascade simulations are found in our earlier work [15,18,19]; here, we give a brief description. Even as these procedures are not meant to replicate the mechanics of cascade formation, nor the structures of real cascades, they do provide a convenient way to establish a range of distinguishable topologies in disordered tetrahedral network structures that are germane to a consideration of amorphization and the structure of the metamict state.

Assemblies comprising 10,000 tetrahedra of the crystalline polymorph precursors were first generated using the appropriate topological assembly rules [12]. Connections between the central 2000 tetrahedra were severed and the tetrahedra randomly rotated and translated, to simulate the stage of a collision cascade at which short-range ordered units reform following initial atomic disordering. These tetrahedra were then reassembled into reconnected structures using the algorithms indicated above. The rules based reassembly of the α-quartz cascade involved rebonding of the 2000 radomized tetrahedra following (so far as possible) imposed α-cristobalite assembly rules. Rules-based reassembly favors establishment of the angular relationships between tetrahedra characteristic of the structure to which the imposed rules apply, in this case the higher temperature polymorph cristobalite, whose use was meant to reflect the elevated temperature within a cooling cascade at the point at which the displaced atoms in the cascade begin to reassemble into structural units. The result has been shown to be topologically disordered structures whose topologies are intermediate between precursor and reassembly-rule polymorphs. The structure thus generated is referred to here as a *quartz cascade/cristobalite reassembly*. A central cube of 500 tetrahedra from these reconstructions was selected for subsequent MD refinement using a periodic boundary condition imposed by periodic replication of this central cube.

Global maximal matching is an algorithm which attempts to establish maximum connectivity by minimizing the total elastic energy stored in Hookeian springs that could be potentially attached between all pairs of matched [SiO_4] tetrahedron vertices. The procedure hence favors connectivity over angular relationships, and the result of its application has been shown [16] to be fully connected topologically disordered reassemblies that, while amorphous, bear strong resemblance to their crystalline precursors. Similar MD refinement was carried out on 500 tetrahedra selected from the centers of maximally matched cascades of identical size in α-quartz and β-cristobalite. We refer to these structures simply as maximally matched *quartz cascade* and *cristobalite cascade*.

As a reference structure, a randomized silica structure was generated by putting 1000 oxygen atoms and 500 silicon atoms into random positions in the MD simulation box using coordinates established by a random number generator. This structure is referred to as *random silica*. All four initial starting configurations were scaled to have the same density of 2200 kg/m^3 within a simulation box size of 2.83 nm on a side.

While topological modeling establishes sensible atom arrangements and supplies a range of desired representative topologies that cannot be obtained by using other modeling methods, including de novo MD, it does not provide realistic atomic coordinates, because the structures have been optimized with, at best, crude Hookeian-spring representations of interatomic potentials. Residual vertex-to-vertex spring lengths remaining in the topological assemblies after elastic energy minimization, in fact, represent distortions of the tetrahedra, whose elastic energy is is not accounted for. MD simulation [20], on the other hand, does provides a vehicle for modeling to a more realistic potential, and in particular provides a vehicle for refining otherwise rather crude topologically modeled structures within their established topologies. The potential function used in this study is that devised by van Beest-Kramer-van Santen (BKS) [21].

Derived from ab initio calculations, the pairwise BKS potential function works surprisingly well for crystalline silica polymorphs [22–24] as well as for vitreous silica

[25–27]. In order to reduce the negative pressure in vitreous silica BKS-modeled with a short-range cutoff of 0.76 nm, the cutoff was reduced to 0.55 nm, with no noticeable structural change observed [25,27]. The long-range Coulombic force was calculated using an Ewald summation with a cutoff of 1.2 nm. Use of a pairwise potential, rather than a three-body function, introduces an apparent anomaly into the Si–Si distance (see Section 3.3) but provides better overall agreement than do three-body potentials with other experimental silica structural parameters [22,24,27].

MD simulations were performed on the topologically modeled structures with periodic boundary conditions at selected equilibration temperatures between 500 and 5000 K for 2.5×10^5 timesteps, followed by cooling to 300 K at a rate of 10 K/ps. The temperature was scaled down every five timesteps to minimize the impact of thermal changes. Additional simulations with 25,000 steps were performed afterwards at 300 K, and configurations were collected over the last 20,000 steps at intervals of 50 steps for structure analysis. The time interval between each timestep was fixed to 2 fs for all the simulations. Since our purpose was not to study cooling procedures per se, but to investigate various topologically possible structures of silicas and compare them to vitreous silica of the same density, we chose constant volume NVT simulations using the Berendsen [28] algorithm. Forcing high temperature glasses to equilibrate under room temperature densities, instead of high temperature ones, permits a structure to adjust to final density at both at high and low temperatures, which would not be possible under constant pressure conditions because of the unavoidably high cooling rate used in MD simulations. A more detailed argument for the advantage of using constant volume simulation can be found elsewhere [27]. In short, constant volume conditions force the structure to equilibrate under constraints closer to those imposed on the more slowly cooled low temperature arrangements.

Minimal closed circuits through connected tetrahedra, known as primitive rings [29], provide a unique description of the topology of crystalline silicas and a useful approach to describing the topologies of amorphous silicas [12]. An efficient primitive ring search algorithm [27] capable of complete ring analysis was used to obtain primitive ring counts up to a ring size of 25. To facilitate comparison to published neutron diffraction data, the total correlation function $T(r)$ obtained from atomic coordinates was broadened, using the method described by Wright [30] and coded by Park [31], with $Q_{\max}(4\pi \sin 2\theta_{\max}/\lambda)$ values of 452 nm^{-1}. Neutron diffraction patterns from simulation structures were also synthesized using established thermal neutron elemental scattering lengths and experimental resolution functions.

3. Results and discussion

MD-equilibration resulted in structures that were essentially fully connected networks of four-coordinated Si tetrahedra (Table 1), even for the quartz cascade/cristobalite reassembly which had been shown previously [18] to be substantially underconnected before equilibration. Other features of the equilibrated structures are discussed in turn below.

Table 1
Bridging oxygen (BO) content, 4-coordinated silicon (Si[4]) content, and potential energies (E_{pot}) for 1500-atom MD-refined random silica, maximally matched quartz and cristobalite cascades, and quartz cascade/cristobalite reassembly as a function of equilibration temperature (T_{eq})

Structure	T_{eq} (K)	BO (%)	Si[4] (%)	E_{pot} (eV/atom)
Random	5000	99.7	99.7	−19.175
Cristobalite	2500	99.8	99.6	−19.187
	3000	99.5	99.8	−19.194
	3500	99.8	100.0	−19.180
Quartz	2500	99.9	99.8	−19.171
	3000	99.6	100.0	−19.191
	3500	99.8	100.0	−19.179
Quartz/cristobalite	500	95.9	95.8	−19.063
	1000	98.5	99.0	−19.108
	1500	99.1	99.6	−19.135
	2000	99.4	98.7	−19.154
	2500	99.8	99.6	−19.157
	3000	99.8	99.6	−19.177
	3500	99.9	99.8	−19.183

3.1. Glass transition temperature

As reported by many investigators [25–27], MD-simulated amorphous silica has a much higher glass transition temperature, $T_g \approx 3000$–4000 K, compared to the experimental value of 1446 K [32] measured for vitreous silica. Many reasons for the discrepancy have been advanced, particularly the extremely high cooling rate and/or finite size of the simulation [25,33,34]. Some recent explorations by us [35] have documented the effects of changes in cooling procedure and simulation size in depressing the glass transition temperature.

In Fig. 1, we plot the enthalpy and potential energy of our random silica simulation as a function of system temperature. The cross-over at low temperature is due to the influence of the negative pressure in the system. There is a bend in the enthalpy plot around 3250 K; the bending is more obvious in the plot of potential energy (which is also the configurational energy) that excludes kinetic energy and the pV term. The bend is presumed due to the system falling out of equilibrium because the relaxation time exceeds the time scale of the cooling process. The bending point can thus be identified as the glass transition temperature T_g. Constant pressure simulations of silica glass also give similar behavior, with the falling-out temperature around 3500 K [26].

Experimentally, different cooling rates lead to different glass transition temperatures T_g for a silica glass system and establish different densities and thermal expansion coefficients. These differences may be associated with differences in medium-range structure, particularly as characterized by different ring complement. The alternative structures may all be similarly energetically stable below T_g.

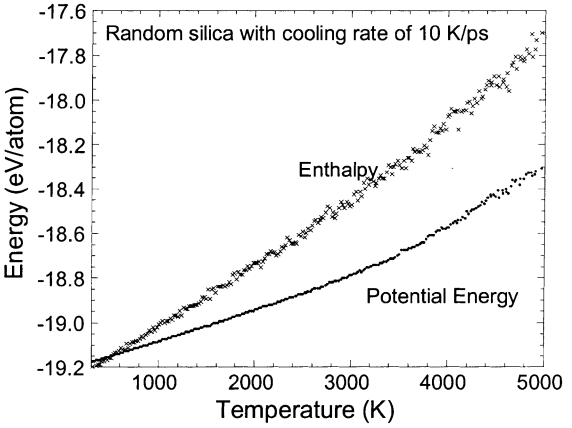

Fig. 1. Plots of enthalpy and potential energy versus system temperature for the random silica MD simulation.

3.2. Structural reconstruction above and below the glass transition temperature

Equilibration of maximally matched α-quartz and β-cristobalite cascades above and below T_g yielded totally different medium-range topologies. Fig. 2 shows the ring statistics for metamict cascades equilibrated at different temperatures, together with the ring statistics for the random silica equilibrated at 5000 K as a comparison. We note that the cascades equilibrated at 3000 K exhibit more prominent distribution peaks in the vicinity of 6- and 8-rings, compared to the ring distributions for cascades equilibrated at 2500 K. Correspondingly, 3000 K-equilibrated cascades also have lower system energies than those of the 2500 K-equilibrated cascades (Table 1). This observation may suggest that, while the thermal

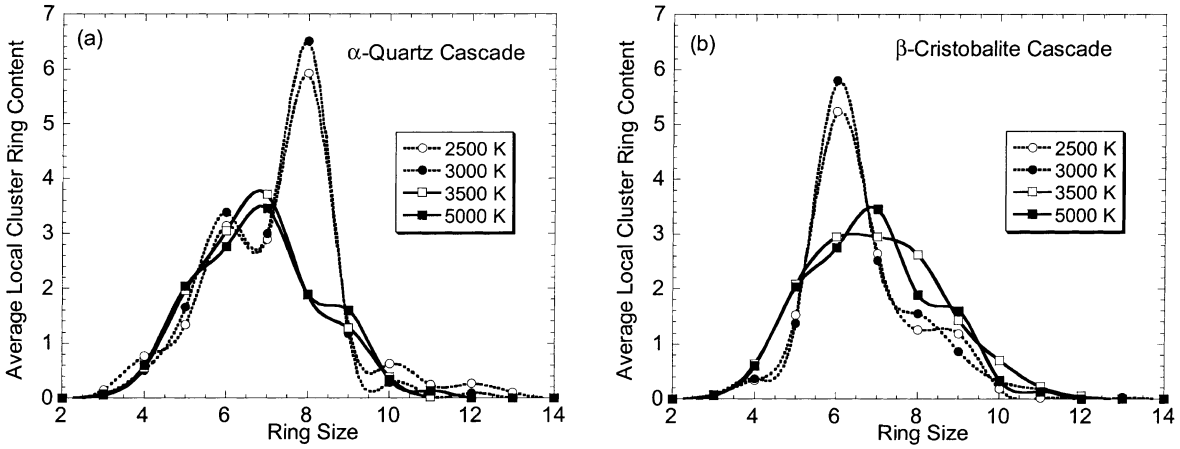

Fig. 2. Distribution of primitive ring content in local clusters of 1500-atom MD-refinement of a 2000-tetrahedron maximally matched (a) α-quartz, and (b) β-cristobalite cascades, equilibrated at three different MD simulation temperatures. The ring distribution of a random silica equilibrated at 5000 K is also plotted as a reference.

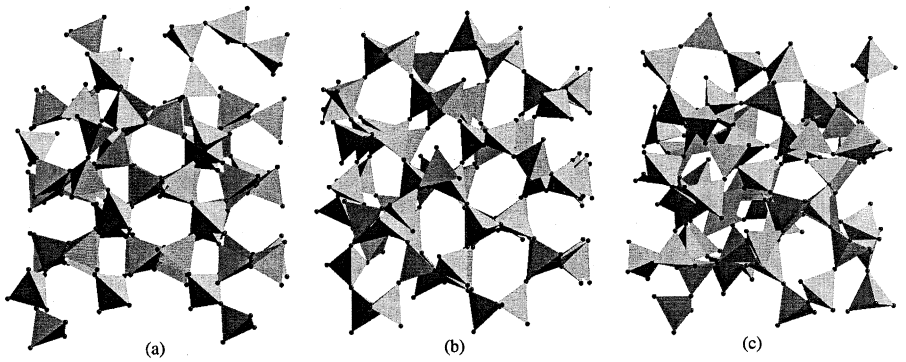

Fig. 3. Central portions of 1500-atom MD-refinements of 2000-tetrahedron cascades in maximally matched (a) α-quartz equilibrated at an MD simulation temperature of 2500 K; (b) β-cristobalite similarly equilibrated at 2500 K, and (c) at 3500 K. The latter reverts to a more random structure, topologically similar to that derived from a random initial starting configuration equilibrated at 5000 K, whose topology is represented in Fig. 2.

energy at 3000 K is not high enough to activate major topological reconstruction in both systems, structures undergo better refinement at 3000 K than do systems equilibrated at 2500 K, with a consequent lowering of system energy. At 3500 K, however, the thermal energy is sufficient for the system to reconstruct. The 3500 K-equilibrated structures all develop ring distributions similar to those in the random silica structure equilibrated at 5000 K (Fig. 2), although their overall system energies increase slightly as compared to their more organized precursors. Nonetheless, it is evident that these structures, with clearly distinguishable ring statistics, are all in metastable states with insignificant differences in system energy.

The maximally matched quartz cascade equilibrated at or below 2500 K yielded about twice as many 8-rings as 6-rings (Fig. 2(a)), reflecting the predominance of 8-rings (40 8-rings, 6 6-rings) in the quartz precursor [12]. By comparison, the maximally matched cristobalite cascade, whose precursor contains only 6-rings [12], exhibited about six times more 6-rings than 8-rings (Fig. 2(b)). Together with the random silica reference (or the cascades equilibrated well above 3000 K), these structures represent three fully connected amorphous silica networks with three distinct topologies. Graphic representations of the three tetrahedral structures are shown in Fig. 3, which more intuitively document the substantial differences in the tetrahedral arrangements and scale of the disorder. The maximally matched metamict structures, while not formally long-range ordered, nevertheless significantly retain the appearance of their crystalline precursors; those appearances differ substantially from that of the random silica. As discussed in Section 3.4, the maximal-match cascade reconstruction is topologically influenced by the surrounding undisturbed material. It may be a fine point whether or not the structures of these cascades correspond to direct impact amorphization.

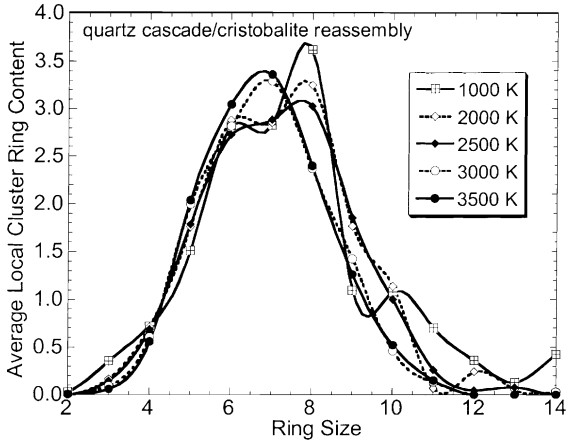

Fig. 4. Distribution of ring content in local clusters of 1500-atom MD-refinement of a 2000-tetrahedron cascade in α-quartz, reassembled with α-cristobalite rules and equilibrated at five different MD simulation temperatures.

A systematic study was carried out on the quartz cascade/cristobalite reassembly with the results shown in Table 1 and Fig. 4. As the equilibration temperature was increased step-wise from 500 K to 2000 K, the number of large rings (>8-rings) decreased steadily, corresponding to progressive elimination of the underconnection of the initial cascade. The cascade exhibited a more equal distribution of 6- and 8-rings (Fig. 4) for equilibration temperatures at or below 2500 K, but still a significantly different ring structure from those obtaining at or above 3000 K or for random silica. Table 1 indicates a lower apparent T_g (between 2500 and 3000 K) than for the maximally matched quartz or cristobalite cascades.

We note that, while maximally matched cascades and random silica in Fig. 2 exhibit significantly different ring

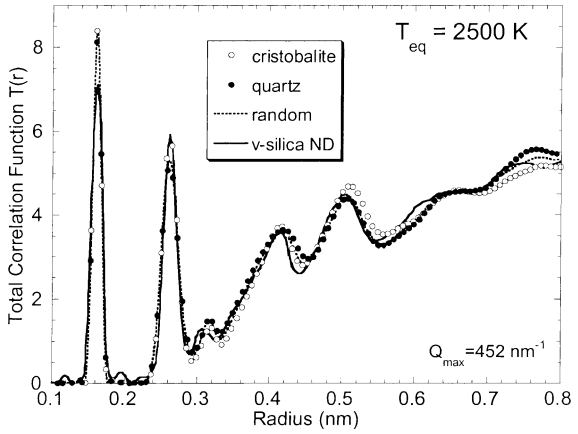

Fig. 5. Total correlation function, $T(r)$, calculated from maximally matched MD-refined collision cascades in quartz and cristobalite, and an MD-randomized silica. Neutron diffraction-derived data for vitreous silica [27] are also plotted for comparison.

structures, the differences in their total correlation functions are rather trivial, as shown in Fig. 5. It is striking to see how insensitive $T(r)$ is to the substantial medium-range structural differences. A similar conclusion is reached in comparing simulated diffraction patterns for the modeled structures, which are virtually indistinguishable (except for the position of the FSDP, Section 3.3).

3.3. Ring statistics and the FSDP

Fig. 2 shows that silicas well-equilibrated at and above 3500 K yield primitive ring statistics with a distribution peaking in the vicinity of 7-rings and shoulders at 5- and 9-rings, yielding an average ring size of 6.8. On the other hand, the density-ring correlation proposed by Hobbs and co-workers [12,17] suggests that silica glass with density of 2200 kg/m^3 should yield an average ring size closer to 6. The slightly higher density of metamict silica (2260 kg/m^3) indeed argues for some larger rings in metamict structures. The discrepancy in ring statistics between the MD simulations and topological arguments for vitreous silica may, however, arise from the fact that the BKS potential function tends to generate an overwide Si–O–Si bond-angle distribution [24,27], as shown in Fig. 6, through over-representation of the Si–Si repulsive interaction. The bond-angle distribution is deemed critical to medium-range structure in vitreous silica networks [27], though Hobbs et al. have pointed out that *no* correlation between Si–O–Si angle and topology or density exists for the crystalline polymorphs of silica [17]. The correspondingly responsible Si–Si distance (the third peak in the vicinity of 0.31 nm in the total correlation function depicted in Fig. 5) for the MD-modeled silica is distinctly larger than that derived from neutron diffraction data for vitreous silica and is thus in error. Therefore, improvement of the potential functions to address the Si–Si distance problem, and thus the Si–O–Si bond-angle distribution, is warranted for better utilization of MD data in understanding the medium-range structure of silica glasses.

Correlation between ring statistics and the FSDP appears more promising. As noted recently by Hobbs and Yuan [19], distinctions in medium-range structure may be better drawn in reciprocal space from the FSDP, which can be used to identify the prominent ring topology contained in disordered structure [36]. Fig. 7(a) illustrates the FSDP in the electron diffraction pattern in α-quartz respectively amorphized by 200 keV electron, 1 MeV reactor neutron, and 150 keV Si^+ ion irradiations, demonstrating that the topology of metamict silica depends on the mode of its production. (The radical shift for the Si^+ ion irradiation reflects non-stoichiometric incorporation of the implanted ion into the amorphized

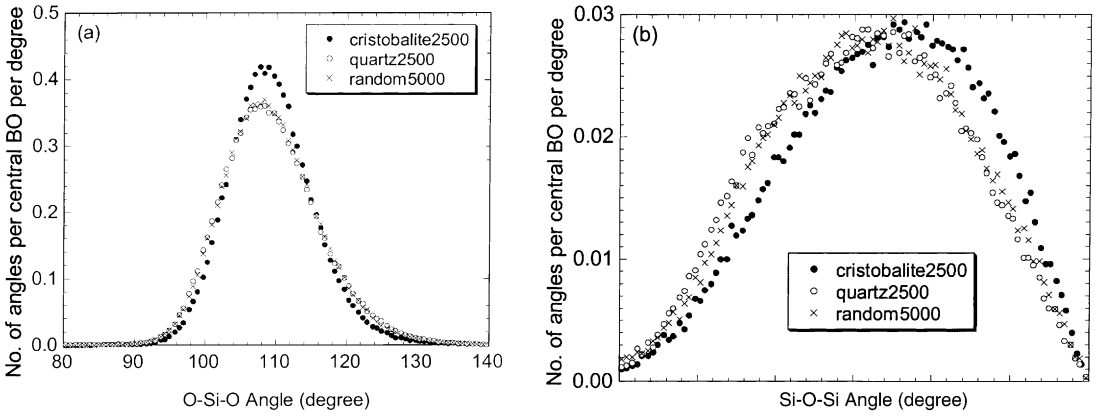

Fig. 6. (a) O–Si–O, and (b) Si–O–Si bond-angle distribution for maximally matched cascades after MD refinements.

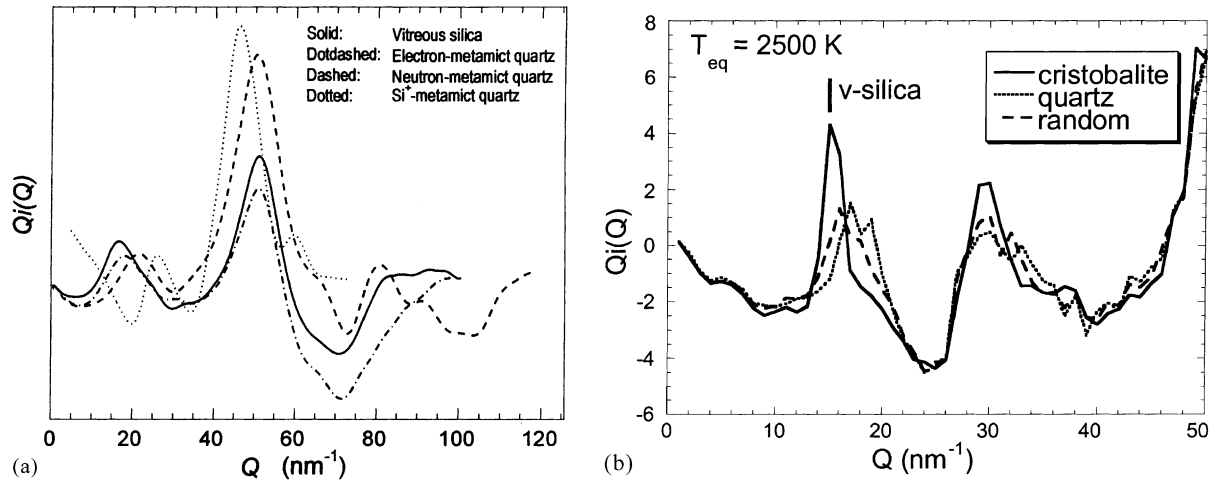

Fig. 7. (a) Angular distribution of electron diffraction intensity from α-quartz fully amorphized by fast electron, fast neutron, and Si^+ ion irradiations [36]; (b) simulated neutron diffraction interference function, deduced from maximally matched MD-refined collision cascades in quartz and cristobalite, and an MD-randomized silica, showing shifts in the FSDP which track corresponding topologies in Fig. 2.

structure.) Fig. 7(b) shows the shift in position of the FSDP in diffraction patterns simulated from the two maximally matched MD-refined cascades and the MD-randomized structure. Reference to the ring statistics in Fig. 2 shows that these shifts in the FSDP correlate with ring statistics. Analogy suggests that, while vitreous silica appears to have a cristobalite-like 6-ring dominated structure, metamict quartz is distinguishably different, with some larger rings.

3.4. The metamict transition in silicas below T_g

Fast neutron irradiation alters the crystalline structure of quartz, as well as the amorphous structure of vitreous silica, by accumulation and overlap of collision cascade events. Experimental studies show that, under neutron irradiation, all crystalline polymorphs (quartz, cristobalite, tridymite) compact and approach the same final density of 2260 kg/m^3 at saturation, while vitreous silica expands to the identical density [3–6]. Other studies show that neutron irradiation transforms several forms of silica to optically isotropic, glass-like structures with virtually identical density, thermal expansion [37], elastic properties [38], and absence of Bragg peaks in X-ray diffraction patterns. Further studies, invoked earlier, have shown that metamict silicas differ from vitreous silica and from pressure-densified silica of comparable density both spectroscopically and energetically [8–10].

It is not unreasonable to expect that different forms of radiation may induce different topologies in metamict structures, because the effective temperature during reconstruction, which governs structural stability and preferences, can differ significantly for different displacive processes. Reconstruction occurring during electron irradiation, which has been shown [39] to arise from accumulation of single-atom radiolytic displacements rather than cascades, arguably occurs at the *ambient* sample irradiation temperature. Room-temperature electron irradiation of silicas could, for example, favor more quartz-like metamict topologies (lower temperature polymorph), on average larger ring sizes, and a FSDP shifted to higher Q than for vitreous silica because of the denser packing of larger rings. Although the effective temperature and duration of the reconstructive phase of real cascades in silica is not known, if it were below the glass transition temperature for vitreous silica ($T_g = 1446$ K [32]) for the major portion of this phase, it is possible that cascade-disordered metamict material may retain some characterizable medium-range structural features of its precursor or at least of the crystalline polymorph most stable at the effective cascade temperature in the reconstructive phase. Reconstruction of a cascade is also strongly influenced by the structure of the surrounding undamaged material, whose topology overlaps that of the cascade, and the precursor structure will thus continue to exert a structural influence until well after cascades have overlapped. This influence is evident in Figs. 3(a) and (b) and has been confirmed in maximally matched simulations by varying the size of the cascade.

While vitreous silica appears to retain its 6-ring structure from the melt, pressure-densified silica may also partially preserve structural elements (in addition to tetrahedra) it possessed before imposition of pressure that are not totally destroyed by the pressure. Most MD-simulated glasses reported in the literature are

generated by a melt-quench approach that inevitably carries over high temperature structures. It is unclear whether metamict silica that is sufficiently irradiated to the *saturation* state should be able to carry over any characteristic structure from its precursor. Should not a unique metamict silica structure be *eventually* reachable from any pure silica with whatever structure after sufficient irradiation from the same source? On the other hand, a topologically mediated reconstruction, determined for example, by preferred assembly rules characteristic of a given reconstruction temperature, could be significantly influenced by precursor structure, as seen in the quartz cascade/cristobalite reassembly exercise, for a long time. Careful evaluation of the FSDP arising from comparable irradiations of different silica polymorphs may be able to decide this point.

4. Conclusions

Topology is central to a description of silica structures and transformations between them. This study has shown that no major topological reconstructions can be effected thermally until the system temperature approaches the glass transition temperature, and that molecular dynamic simulation below the glass transition can provide fully connected tetrahedral networks which largely preserve the characteristic topologies of starting configurations. It was also found that amorphous silicas can be constructed with substantially different medium-range structures (as characterized by ring topologies) that are metastable at room temperature with little difference in system energy. The total correlation function is strikingly insensitive to these differences in medium-range structure and exhibits only trivial differences in systems with significantly different ring statistics.

Since vitreous silica inherits topological features from its melt, it is not totally topologically disordered. Irradiation-induced metamict silicas may exhibit more or less – but in any event, *different* – topological disorder than exists in vitreous silica, and several disordering and reconstruction algorithms were investigated to generate a range of possible topologies. Their topological differences were reflected in corresponding differences in the position of the first sharp peak in diffraction from the structures. Although the topological features retained by or developing in real metamict silicas are still not clear at this point, careful study of the first sharp peak may provide some insight into their identities.

Acknowledgements

The authors acknowledge the support by the Office of Basic Energy Sciences, US Department of Energy, under DOE grant DE-FG02-89ER45396. Thanks also go to Professor Alastair N. Cormack of Alfred University for his advice in the molecular dynamics simulations.

References

[1] W.J. Weber, R.C. Ewing, C.A. Angell, G.W. Arnold, A.N. Cormack, J.M. Delaye, D.L. Griscom, L.W. Hobbs, A. Navrotsky, D.L. Price, A.M. Stoneham, M.C. Weinberg, J. Mater. Res. 12 (1997) 1946.
[2] W.J. Weber, R.C. Ewing, C.R.A. Catlow, T. Diaz de la Rubia, L.W. Hobbs, C. Kinoshita, Hj. Matzke, A.T. Motta, M.A. Nastasi, E.H.K. Salje, E.R. Vance, S.J. Zinkle, J. Mater. Res. 13 (1998) 1434.
[3] E. Lell, N.J. Kreidl, J.R. Hensler, Prog. Ceram. Sci. 4 (1966) 1.
[4] M.C. Wittels, A.F. Sherrill, Phys. Rev. 93 (1954) 1117.
[5] M.C. Wittels, Philos. Mag. 2 (1957) 1445.
[6] W. Primak, Phys. Rev. 110 (1958) 1240.
[7] R.C. Ewing, Nucl. Instrum. and Meth. B 91 (1994) 22.
[8] A. Navrotsky, Trans. ACA 27 (1991) 1.
[9] S. Susman, K.J. Volin, R.C. Liebermann, G. Gwanmesia, Y. Wang, Phys. Chem. Glasses 31 (1990) 144.
[10] R.J. Hemley, K.K. Mao, P.M. Bell, B.O. Mysen, Phys. Rev. Lett. 57 (1986) 747.
[11] L.W. Hobbs, J. Non-Cryst. Solids 192/193 (1995) 79.
[12] L.W. Hobbs, C.E. Jesurum, V. Pulim, B. Berger, Philos. Mag. A 78 (1998) 679.
[13] A.C. Wright, J. Non-Cryst. Solids 179 (1994) 84.
[14] L.W. Hobbs, C.E. Jesurum, B. Berger, in: P.M. Duxbury, M.F. Thorpe (Eds.), Rigidity Theory and Applications, Plenum, New York, 1999, p. 191.
[15] L.W. Hobbs, C.E. Jesurum, V. Pulim, Mater. Sci. Eng. A 253 (1998) 16.
[16] L.W. Hobbs, C.E. Jesurum, A. Coventry, V. Pulim, R. Schwartz, B. Berger, in: Y.-W. Chung, D.C. Dunand, P. Liaw, G.B. Olson (Eds.), Advanced Materials for the 21st Century: the Julia R Weertman Symposium, TMS, Warrendale, PA, 1999, p. 475.
[17] L.W. Hobbs, C.E. Jesurum, B. Berger, in: J.-P. Duraud, R.A.B. Devine, E. Dooryhee, (Eds.), Structure and imperfections in amorphous and crystalline silica, Wiley, London, 2000, p. 1.
[18] C.E. Jesurum, V. Pulim, L.W. Hobbs, Nucl. Instrum. and Meth. B 114 (1998) 25.
[19] L.W. Hobbs, X. Yuan, in: G. Pacchioni, L. Skuja, D.L. Griscom (Eds.), Defects in SiO_2 and Related Dielectrics: Science and Technology, Kluwer, Netherlands, 2000, p.37.
[20] A.N. Cormack, Y. Cao, in: B. Silvi and P.D' Arco (Eds.), Modelling of Minerals and Silicated Materials, Kluwer, Netherlands, 1997, p. 227.
[21] B.W.H. van Beest, G.J. Kramer, R.A. van Santen, Phys. Rev. Lett. 64 (1990) 1955.
[22] M. Hemmati, C.A. Angell, J. Non-Cryst. Solids 217 (1997) 236.
[23] G.J. Kramer, N.P. Farragher, B.W.H. van Beest, R.A. van Santen, Phys. Rev. B 43 (1991) 5068.
[24] J.S. Tse, D.D. Klug, J. Chem. Phys. 95 (1991) 9176.
[25] K. Vollmayr, W. Kob, K. Binder, Phys. Rev. B 54 (1996) 15,808.

[26] J. Horback, W. Kob, Phys. Rev. B 60 (1996) 3169.
[27] X. Yuan, Ph.D. Dissertation, Alfred University, Alfred, NY, 1999.
[28] H.J.C. Berendsen, J.P.M. Postma, W. van Gunster, A. DiNala, J.R. Haak, J. Chem. Phys. 81 (1984) 3684.
[29] C.S. Marians, L.W. Hobbs, J. Non-Cryst. Solids 124 (1990) 242.
[30] A.C. Wright, in: C.J. Simmons, O.H. El-Bayoumi (Eds.), Experimental Techniques of Glass Science, American Ceramic Society, Westerville, OH, 1993, p. 205.
[31] B. Park, Ph.D. dissertation, Alfred University, Alfred, NY, 1998.
[32] C.A. Angell, J. Phys. Chem. Solids 49 (1988) 863.
[33] A.N. Cormack, B. Park, X. Yuan, in: Proceedings of the Fifth European Society on Glass Science Technology, Prague, Czech Republic, 1999.
[34] J. Horbach, W. Kob, K. Binder, Phys. Rev. E 54 (1996) 5897.
[35] X. Yuan, V. Pulim, L.W. Hobbs, Refinement of topologically modeled cascade-amorphized silicas using molecular dynamics simulation, in: G.E. Lucas, L. Snead, M.A. Kirk, Jr., R.G. Elliman (Eds.), Microstructural Processes in Irradiated Materials, Mater. Res. Soc. Symp. Proc., 2001, in press.
[36] L.-C. Qin, L.W. Hobbs, J. Non-Cryst. Solids 192/193 (1995) 456.
[37] I. Simon, J. Am. Ceram. Soc. 41 (1958) 116.
[38] G. Mayer, M. Lecomte, J. Phys. (Paris) 21 (1960) 846.
[39] L.W. Hobbs, M.R. Pascucci, J. Phys. (Paris) 41 (C6) (1980) 237.